Published in final edited form as:
Arch Microbiol. 2014 December ; 196(12): 881–890. doi:10.1007/s00203-014-1027-6.

Composition and occurrence of lipid droplets in the cyanobacterium *Nostoc punctiforme*

Anantha Peramuna and **Michael L. Summers***

Abstract

Inclusions of neutral lipids termed lipid droplets (LDs) located throughout the cell were identified in the cyanobacterium *Nostoc punctiforme* by staining with lipophyllic fluorescent dyes. LDs increased in number upon entry into stationary phase and addition of exogenous fructose indicating a role for carbon storage, whereas high-light stress did not increase LD numbers. LD accumulation increased when nitrate was used as the nitrogen source during exponential growth as compared to added ammonia or nitrogen–fixing conditions. Analysis of isolated LDs revealed enrichment of triacylglycerol (TAG), - tochopherol, and C17 alkanes. LD TAG from exponential phase growth contained mainly saturated C16 and C18 fatty acids whereas stationary phase LD TAG had additional unsaturated fatty acids characteristic of whole cells. This is the first characterization of cyanobacterial LD composition and conditions leading to their production. Based upon their abnormally large size and atypical location these structures represent a novel sub-organelle in cyanobacteria.

Keywords

Neutral lipid droplet; cyanobacteria; triacylglycerol; -tochopherol; alkane production

Introduction

Intracellular lipid-containing structures are found in many cell types in nature. These subcellular organelles are found in the cell cytoplasm of most eukaryotic organisms, within eukaryotic plastids, and in some bacteria (Murphy and Vance 1999). They have been designated various terms depending upon the field of study, including lipid inclusions, lipid bodies, lipid droplets, lipid globules, adiposomes, granules, oleosomes, plastoglobules, or oil bodies. Due to the majority of literature referring to lipid droplets (LDs) and suggestions to adopt this term (Farese and Walther 2009; Murphy and Vance 1999), LDs will be used as a general descriptor for the cyanobacterial structure central to this work.

LDs of all types are proposed to have a neutral lipid core surrounded by a lipid mono-layer membrane containing polar or charged headgroups (Murphy 2012). The current model of eukaryotic cytosolic LD biogenesis is that they bud or “blister” off of the outer leaf of the endoplasmic reticulum (ER) due to accumulation of neutral lipids between the leaflets of the

*Corresponding author: Mailing address: Department of Biology, California State University Northridge, 18111 Nordhoff St. Northridge, CA 91330-8303 Phone: (818) 677-7146 Fax: (818) 677-2034 Michael.l.summers@csun.edu.

Conflict of interests The authors declare that they have no conflict of interest.

phospholipid bilayer (Khandelia et al. 2010; Khandelia et al. 2010; Wang et al. 2009). LDs are covered by scaffolding proteins, such as oleosins in plants (Chapman et al. 2012) and perilipins in animal cells (Yang et al. 2012), which contribute to LD formation and stabilization (Jacquier et al. 2013). Recently the view of cytosolic LDs as static storage structures has changed with the realization that some LDs may have more dynamic roles, such as for lipid biosynthesis, membrane trafficking, signaling, and protein degradation (see (Yang et al. 2012) and references therein). Alterations of LD dynamics in animal cells have been linked to certain metabolic diseases such as obesity, type 2 diabetes mellitus, and atherosclerosis (Maeda et al. 2005).

Oleaginous algal species have received much attention due to the potential use of triacylglycerols (TAGs) that are stored in algal LDs as a “green” fuelstock for biodiesel production (Hu et al. 2008). The TAGs in algae and plants are thought to arise from de novo fatty acid synthesis in the chloroplast (Moellering et al. 2009). The resultant fatty acids can be used by or stored in the chloroplast as LDs, or following export into the cytosol, can be used in the endoplasmic reticulum (ER) to sequentially acylate glycerol-3-phosphate and produce diacylglycerol (DAG). DAG can then serve as an immediate precursor for the synthesis of either membrane lipids or storage TAG that is deposited in ER-derived cytoplasmic LDs (Fan et al. 2012). In the algae *Chlamydomonas,* the DAG precursor of TAG is of chloroplast origin, and abnormally large LDs accumulate in both the chloroplast and the cytosol in algae supplemented with acetate (Goodson et al. 2011), in a mutant incapable of starch production (Fan et al. 2012), or when growth is inhibited by nitrogen starvation (Miao and Wu 2006).

Lipid-containing structures ranging from 30 nm to 5 μm in diameter, known as plastoglobules (PGs), occur in all types of plant plastids (Kessler and Vidi 2007). Chloroplast PGs are typically round/oval in shape and contain mainly TAGs and prenylquinone compounds [-tocopherol (vitamin E; a protector against oxidative damage), phylloquinone (vitamin K1) and plastoquinone (electron carrier in electron transfer chains)], with smaller amounts of sterol esters (Kessler and Vidi 2007; Piller et al. 2012). In chloroplasts, PGs are mainly attached to thylakoid membranes near their curved surfaces, with smaller numbers in the stroma. The current model of PG formation in chloroplasts is similar to budding or “blistering” from the outer leaf of the ER described for eukaryotic cells, except in this case PGs originate from the cytoplasmic side of the chloroplast thylakoid membrane. Owing to the endosymbiotic origin of plant and algal chloroplasts, it is likely that PGs of chloroplasts are related to the LDs of cyanobacteria.

Small 50-100 nm diameter LDs have been described sporadically in cyanobacterial literature, mainly in association with electron microscopy studies (Edwards et al. 1968; Wolk 1973; van de Meene et al. 2006) and little is known about their function or formation. This work describes the presence of large LDs in the filamentous cyanobacterium *Nostoc punctiforme,* and characterization of their expression and lipid composition.

Materials and methods

Strains and growth conditions

N. punctiforme PCC 73102 cultures were grown in 125 ml Erenmeyer flasks shaking at 120 rpm at 25°C under 13-15 μmol photons s^{-1} m^{-2} from cool white fluorescent lights using the medium of Allan and Arnon (Allen and Arnon 1955), diluted four fold. Flasks were supplemented with one of the following additions (pH 7.8); 5 mM MOPS 2.5 mM Ammonia (MA), 5 mM MOPS 2.5 mM $NaNO_3$ 2.5 mM KNO_3 (MN), 5 mM MOPS 2.5 mM $NaNO_3$ 2.5 mM KNO_3 /50 mM Fructose (MNF) or 5 mM MOPS only. MA stationary phase cultures were supplemented with ammonia for lipid area counting, but not supplemented in experiments for lipid droplet composition from late stationary cultures that should be regarded as dense nitrogen-fixing cultures.

For lipid droplet accumulation determination, triplicate cultures were grown in MOPS, MN, or MNF and sampled during log phase (3.8-5.1 μg Chla/ml) or stationary phase (31-50 μg Chla/ml) for staining and visualization. To determine if lipid formation changed in response to high light, wild type cells were grown in MN under standard light conditions (13-15 μmol s^{-1} m^{-2}) until late log phase (6.1-7.3 μg Chla/ml) a set of triplicate cultures (biological) were exposed to high light (~100 μmol s^{-1} m^{-2}) for 3 or 12 days while a second set of biological triplicates were allowed to grow under the normal light prior to staining and visualization.

Lipid droplet staining and analysis

Lipid droplets were stained using borondipyrromethene difluoride (BODIPY) 505/515 (Invitrogen Molecular Probes, Carlasbad, CA) using 1 μl of a 10 M stock solution, prepared in 100% DMSO, per 20 μl of cell culture at a concentration of 5 μg Chla/ml. Cells were incubated in the dark for 15 minutes at room temperature prior to visualization under a cover slip atop a 1% agarose gel pad. Micrographs were obtained with a Leica LAS AF confocal laser microscope, using a 488 nm laser excitation line and a window of 510-550 nm for visualization. Z stacks were performed on each filament with line averaging set at 4. A maximum projection was performed to combine the Z-stacks for each filament into a single image for analysis.

Isolation of lipids droplets

A previously reported method (Ding et al. 2012) for isolation of lipid droplets was modified to isolate lipid droplets from cyanobacteria. *N. punctiforme* pellets containing 400 or 800 g Chla of late stationary phase or exponential phase cultures, respectively, initially grown with MA were washed twice with buffer A (25mM Tris-HCl, 250mM sucrose, pH 7.8), suspended in 20 ml of the buffer A and lysed by three passes through a French pressure cell at 100 MPa. Homogenized cells were mixed with equal amount of buffer A, loaded into ultracentrifuge tubes, and 2 ml of buffer B (20mM Tris-HCl, 100mM KCl, 2mM $MgCl_2$, pH 7.8) or water was layered on top. Cells were centrifuged at 135,000 Xg for 100 minutes at room temperature using a swinging bucket rotor. The top layer containing neutral lipid droplets was transferred to another centrifuge tube, mixed with four volumes of buffer A,

overlaid with buffer B as before, and the top-most layer harvested after centrifugation at 135,000 x g for 3 hours.

Quantifying Lipid Droplet Formation

The percentage area of LDs per cell was measured from digital images using the software Image J (www.http://imagej.nih.gov). Area of the lipids stained by Bodipy was measured by tracing the outline of the lipid droplets using the freehand selection function and measuring the pixel area within the chosen area. Cell area was determined similarly using outlines of the cell periphery. Percentage area occupied by LDs per cell was determined by dividing the pixel area of the lipids by pixel area of the cell and multiplying by 100.

Identifying the Lipid Classes and Fatty Acids in Lipid Droplets

LD's were isolated from the MA grown late stationary phase cultures (n=3). Isolated lipid droplets from the top fraction and the pellet were extracted using 5 ml iso-octane and ethyl acetate (75/25, V/V) and dried under a nitrogen gas stream (Hutchins, 2008). Dried lipid from the top fraction and the pellet were dissolved in 50 μl of Hexane/ Ether/ Acetic acid (80/20/1, V/V/V) and spotted onto silica coated thin layer chromatography (TLC) plates (SIGMA – ALDRICH; Cat#2737B25) that were pre-washed with chloroform. Following separation with Hexane/ Ether/ Acetic acid (80/20/1, V/V/V) lipids were visualized using iodine vapor. Vegetable oil was used as the triacylglycerol (TAG) standard; diacylglycerol (DAG) standards and charged lipid standards were obtained from Avanti Polar Lipids, Inc. Iodine stained spots on TLC plates were scraped off after iodine has evaporated, extracted with hexane and either injected directly or after conversion to FAME's.

A fraction of the dried lipids were dissolved in chloroform and analyzed using SHIMADZU/ GCMS-QP2010S gas chromatograph-mass spectrometer (GC-MS) equipped with a Rxi-5Sil MS column (0.25mm id x 30m. 0.10 μm film thickness cat#13608) held at 180°C for 1 minute, increased to 300°C at 12°C min^{-1}, with a 300°C final temperature maintained for two minutes. Helium was used as the carrier gas and 1 ul of sample was injected in split mode (1:50). MS detector voltage was set at 0.25 kV, and the samples were identified using NIST11/NIST11s libraries. The other fraction of the dried lipids were converted to fatty acid methyl esters (FAMEs) by saponification of the dried extracted lipids with 1 ml of 1N KOH in anhydrous methanol and heating at 80°C for 30 minutes. Methyl esterization was accomplished by adding 1 ml of BCL_3-Methanol (12% W/W) and heating 100°C for 10 minutes. After cooling, 1 ml water and 1 ml hexane was added and vortexed violently for 1 minute to extract fatty acid methyl esters (FAMEs) in the non-polar solvent. The upper organic layer was removed and dried under a stream of N_2 gas. FAMEs were re-dissolved in hexane and analyzed by GC-MS using a Restek SHRX1-5MS column (0.25mm id x 30m. 0.25 μm film thickness) as above. Identifications were confirmed using NIST11/NIST11s libraries and commercial FAME standards (RESTEK/ Cat#35066).

RESULTS

Discovery of lipid droplets by fluorescence staining

After staining *N. punctiforme* with a BODIPY dye specific for neutral lipids and visualization by fluorescence or confocal laser microscopy, densely staining spherical droplets with an average diameter of 310 nm ± 16 nm (n=20) were identified (Fig. 1A and B). Droplets stained in vivo with HCS LipidTOX™ green neutral lipid stain gave identical results (Fig. 1C). Since these dyes specifically stain uncharged lipids, the densely staining inclusions were tentatively identified as neutral lipid droplets, and experiments were initiated to study them further. Staining with BODIPY occurred within seconds and fluorescence was stable for at least 60 minutes. Membranes surrounding the cell were only stained if excess dye was used. Without staining lipid droplets could not be reliably discerned from other cytoplasmic components using brightfield, DIC, or phase contrast microscopy. Lipid droplets were also observed in akinetes, heterocysts and hormogonia (data not shown). On very rare occasions filaments exhibiting high numbers of LDs per cell were observed (Fig. 1B, bottom filament).

Changes in lipid droplet accumulation due to growth condition and growth phase

In an attempt to find conditions promoting LD formation, the presence of LDs were measured under various growth conditions and compared at the exponential vs. stationary phase of growth. For these measurements, the percent of the cell area containing LDs were obtained from 2D-projections of confocal Z-stacks as a basis of comparison. This method allows visualization of all LDs by combining the different focal planes of the cell into one image, but of necessity, will underestimate the amount in cells containing high numbers of overlapping LDs.

Exponentially growing vegetative cells under nitrogen fixing conditions exhibited the lowest percent of LD area (0.92 ± 0.11%), followed by ammonia (1.39 ± 0.35%) and nitrate (2.17 ± 0.24%) growth (Fig 2A). The highest neutral lipid production in log phase cultures was observed when nitrate-grown cultures were supplemented with fructose (3.13 ± 0.23%), where they exhibited significantly higher amounts of lipid droplets than when grown on nitrate alone ($p=0.008$).

LD accumulation increased as the cells transition from exponential to stationary phase (Fig. 2). Cultures in stationary phase exhibited higher levels (area ranging from 3-4%) with the exception of the nitrate culture supplemented with fructose (2.73 ± 0.26%). This apparent decline in lipid droplet production was a result of increased cell size of fructose-supplemented stationary cells (ave. cell width/length = 4.8 ± 0.16/5.63 ± 0.15 μm relative to the 3.56 ± 0.04/4.05 ± 0.18 μm observed for nitrate alone in stationary) and not to a decrease in lipid droplet area (Fig. 2B). Based upon area measurements from digitized photomicrographs, LD area per cell appears to reach a maximum for stationary cultures and fructose-supplemented cultures regardless of the growth phase (Fig. 2B). As cultures went into late stationary, more LD are per cell was observed (data not shown). LD area per cell increased during stationary phase 1.8-fold in nitrate, 2.4-fold in cultures initially grown in ammonia that transitioned to nitrogen-fixing conditions, and 3.3-fold in steady-state nitrogen

fixation conditions (Fig. 2A). Cells grown with nitrate and supplemented with fructose were not statistically different ($p = 0.26$) in lipid area per cell upon entering the stationary phase of growth due to increased cell size as mentioned above.

Due to the frequently overlapping occurrence of LDs within a cell, the average number of LDs per cell was obtained using calculated estimates from digitized data. The average diameter of distinct non-overlapping individual LDs (n = 100) obtained from confocal micrograph projections of exponentially growing MOPS-only grown cells (290 nm ± 4.8) was similar to that observed for these during stationary phase (307 nm ± 4.6). Using these values, the total area of LDs per cell was converted to number of LDs per cell as a best approximation. The calculated results indicated an average of 1.1 LD per cell for log phase growing in medium containing ammonia, 5.0 per cell for stationary phase cultures previously grown in ammonia that had switched to fixing their own nitrogen, 2.9 per cell for log phase cultures growing in medium containing nitrate, 5.5 per cell for stationary phase cultures grown in nitrate, 5.7 per cell for log phase cultures growing in nitrate and supplemented with fructose, and 5.6 per cell for stationary phase cultures grown with nitrate and fructose. Assuming a single LD of 300 nm diameter has a volume of 0.0141 μl^3, with the average volume of a cell being ~65 μm^3, the percent of a cells volume occupied by LDs ranges from ~0.02 to 0.13% of the cells volume.

To see if LD formation changed following damage to the photosynthetic apparatus, cultures were exposed to high light conditions over six times higher (80-100 $\mu mol\ s^{-1}\ m^{-2}$) than the normal for 4 and 12 days before staining and visualization. Cultures appeared stressed based on bleaching compared to those under normal illumination. Cells grown under MN conditions in normal light for four days in stationary exhibited 4.3 ± 0.45% LD area whereas the highlight treated cells exhibited an insignificant increase to 4.6 ± 0.47 (n = 100 for all samples). Cells exposed to high light for 12 days decreased in LD content to 3.8% area ± 0.45 as compared to 6.7% ± 0.46 for the late stationary cells under normal light.

Enrichment of TAG containing saturated fatty acids and -tocopherol in LDs

Following ultra-centrifugation of a crude lysate in a sucrose step gradient, a less dense yellow layer appeared floating atop the sucrose. It was hypothesized that these were lipid based on density (lipid density from cyanobacteria is ~0.83 (Selvan et al. 2013)). The top fraction contained small droplets that stained with Bodipy and were similar in size (305 nm ± 14 nm, n=20) to that of the neutral lipid droplets inside living cells (Figure 1D and E). Lipid droplets in the top-most fraction as well as cellular debris in the sucrose gradient ultracentrifuge pellet were extracted using iso-octane/ethyl acetate (75/25 V/V). This extraction system (Hutchins et al. 2008) was more effective in our hands for extraction of neutral lipids than that of Bligh & Dyer (Bligh and Dyer 1959), likely due to the inclusion of iso-octane that has a low relative polarity which makes it a better solubilizing agent for neutral lipids.

The thin layer chromatography system using hexane/ether/acetic acid (80/20/1) as the mobile phase prevented charged (Fig. 3, lane 1) lipid migration and kept chlorophyll and an unidentified red pigment near the origin, thus avoiding their potential co-migration with more-neutral lipids with higher mobility. The polar lipids mono- and

digalactosyldiacylglycerols (MGDG and DGDG) also remained at the origin (data not shown). Following visualization with iodine vapor, LDs appeared to contain reduced levels of charged and polar lipids relative to the other lipids in the sample that stayed near the origin as compared to lysed cells (Fig. 3, lanes 5 & 6). These are likely the 4 major glycerolipids found in cyanobacteria: polar MGDG and DGDG and charged sulphoquinovosyldiacylglycerols and phosphatidylglycerols (Sheng et al. 2011; Boudière et al. 2014).

Only two types of lipids appeared to be over-represented in the LD enriched fraction (asterisks in Fig. 3, lanes 5 & 6). The upper spot migrated similar to the TAG standard, and produced only C16:0 and C18:0 FAMEs identified by GC-MS following saponification and methyl esterization of the excised spot. The lower spot was also excised, subjected to GC-MS analysis, and identified as -tocopherol. One high mobility spot near the solvent front of the TLC plate contained a mix of heptadecane and squalene. The identity of the upper-most spot and a red pigment migrating below the alpha-tochopherol remain to be determined. Samples of un-derivitized LD lipid extracts subjected to GC-MS analysis identified squaline, alpha-tochoperol, and C17 alkanes.

To gain insight into LD fatty acid composition, whole cells, purified LDs, and pellets containing lysed cell material remaining after LD removal were saponified and derivatized into fatty acid methyl esters (FAMEs) for analysis by GC/MS (Fig. 4). The elution time of FAME samples from *N. punctiforme* matched those of commercial FAME standards as well as predictions from the mass spectrometer compound library (NIST11 and NIST11s) following mass spectrometry. These results indicate that *N. punctiforme* lipids contain six major fatty acids: C16:0 [Hexadecenoic acid (Palmitic acid)], C16:1 [9-Hexadecenoic (Palmitoleic) acid], C18:0 [Octadecanoic (Stearic) acid], C18:1- [both 9- Hexadecenoic (Oleic) and (E)-Octadec-11-enoic (Vaccenic) acid], C18:2 [9,12- Octadecadienoic (Lenolelaidic) acid] and C18:3 [9,12,15- Octadecatrienoic (Linolenic) acid]. Major amounts of a C17 alkane was also detected along with small amounts of several unconfirmed compounds; squalene (97% confidence), gamma-Dodecalactone (86% confidence), 10-Methylundecane-4-olide (85% confidence). The latter was only apparent in the ultracentrifuge pellet and was absent in the LD fraction. Trace amounts of phytol acetate (91% confidence) and 3,7,11,15-tetramethyl-2-hexadecen-1-ol (92% confidence) and C14:0 FAME were detected. Butylated hydroxytoluene (Fig. 3, lane 3) was found in many extracted spots and determined to be a contaminant in the solvents used for TLC analysis.

The relative proportions of fatty acids in whole cells (Fig. 4A) roughly paralleled that of ultracentrifuge pellets obtained from similarly grown exponential (Fig. 4B, light bars) and late stationary (Fig. 4C, light bars) phase cultures. Exponential phase cultures contained high proportions of C16:0 fatty acids whereas during stationary phase C16:1 and 18:2 were the dominant species present. In stationary phase cultures C18:3 fatty acids seem to be replaced by C18:1 (vaccenic acid) fatty acids. The proportion of C17 alkane also increased during stationary phase in comparison to exponentially grown cells.

The relative proportions of fatty acids in LDs were different from whole cells under each growth phase, and also varied between LDs obtained from the two growth phases. During

exponential growth LDs contained primarily C16:0, C18:0 and C17 alkanes, with smaller amounts of C16:1 fatty acids (Fig. 4B, dark bars). Unsaturated C18's were present only in trace amounts. During late stationary phase LDs were also enriched for C16:0, C18:0 and C17 alkanes, but also contained significant amounts of C16:1 and all three species of unsaturated C18's, especially C18:2 that was also observed in whole cell and pellet fraction lipids (Fig. 4C, dark bars). TAG spots from LD and pellet fractions were also excised from TLC plates, saponified and converted into FAME's and were found to contain only C16 and C18 saturated FAMEs. Together, these results indicate that LDs are enriched for alpha-tochoperol, C17 alkanes, and TAG containing C16:0 and C18:0 fatty acids.

Discussion

BODIPY has been shown to specifically stain neutral lipids (Cooper et al. 2010) and used to identify LDs in bacteria, algae and fungi (Kuroiwa et al. 2012). Interestingly, no lipids were observed in the cyanobacterium *Anabaena flos-aquae* using this stain (Kuroiwa et al. 2012), however cyanobacterial LDs have been mentioned repeatedly in the literature as spherical small features in electron micrograph. The sizes of cyanobacterial LDs have been observed to be 30-90 nm in *Simploca muscorum* (Pankratz and Bowen 1963), 40-100 nm in *Synechococcus lividus* (Edwards et al. 1968), 50-70 nm in *Synechocystis* sp. strain PCC 6803 (van de Meene et al. 2006), and similarly small in size in *Agmenellum quadruplicatum* (Nierswicki-Bauer et al. 1983). Plastoglobules (PGs), the analogous low-density lipoprotein bodies found in chloroplasts, have an average diameter of 50-100 nm in vegetative leaf tissue, but can increase up to several micromenters in diameter in response to abiotic stress conditions (Bréhélin and Kessler 2008). The ~300nm in diameter size LDs found in *N. punctiforme* are therefore the largest yet found among cyanobacteria, however additional observations using electron microscopy will be required to see if the LDs observed in this work are actually due to closely associated clumps of smaller ones linked together by a mono-layer coating of lipids as has been observed for herbaceous plant PGs (Austin et al. 2006). We have isolated LDs as free entities following cell lysis (Fig. 1D & E) indicating they can exist free of membranes, but cannot rule out the possibility that they were initially attached and subsequently broken free from membranes during cell lysis. If however clumps of smaller LDs exist *in vivo*, it seems reasonable to expect that smaller LDs would be enriched in purified samples instead the ~300 nm ones obtained that were almost identical in size to those observed *in vivo* (Fig. 1).

The location and number of the smaller-sized LDs previously observed within cyanobacteria also varies from that observed in *N. punctiforme*. Cyanobacterial LDs have been observed around the edges of cells near thylakoid membranes adjacent to septal crosswalls (Pankratz and Bowen 1963), around the periphery of the cell between the outermost thylakoid membrane and the cytoplasmic membrane with far fewer between internal thylakoid membranes (Edwards et al. 1968; Nierswicki-Bauer et al. 1983), and at the intersection of the outermost thylakoid membrane and cytoplasmic membrane (van de Meene et al. 2006). In contrast, 3-D images of stained LDs within *N*. punctiforme cells created from confocal z-stacks and their projections used for area analysis (Fig. 1) revealed no bias for location of LDs to the periphery of cells. The 3-6 LDs per cell observed by staining in stationary phase *N. punctiforme* fell far short of the 17-20 reported for smaller LDs observed in electron

micrographs (Nierswicki-Bauer et al. 1983; van de Meene et al. 2006) except perhaps for rare members of the population exhibiting large numbers of LDs (Fig 1). If indeed these are analogous structures, it can be hypothesized that fewer LDs are needed in *N. punctiforme* due to their larger size. It has been proposed that there are two strategies for PG formation in chloroploasts as leaves age. Spinach and other herbaceous plants increase the number of small PGs up to several hundred, where as older leaves of beech, oak, or *Ficus* trees produce smaller numbers of large PGs 400-2,000 nm in diameter (Lichtenthaler 2007). It is possible that various species of cyanobacteria have similar differences.

Work done on plastid PGs have identified fibrillin proteins hypothesized to interact with charged or polar head groups of mono-layer external lipids surrounding PGs that act to stabilize these structures in plant plastids (Deruere et al. 1994). Mutation of two fibrillin orthologs in *Synechocystis* 6803 resulted in the appearance of large heterogeneous inclusion bodies and a light sensitive phenotype, supporting their role in adaptation to high light even though they could not be localized to LDs (Cunningham et al. 2010). To see if high-light damage of the thylakoid membranes could increase LD production, cultures were exposed to light at intensities high enough to cause visible bleaching. Lipid droplet formation did not significantly change when wild type cells are exposed to high light for 4 days, and cells that were exposed to high light for 12 days had fewer LD's compared to the cells grown under normal light conditions. If these cyanobacterial LDs played an active role in lipid protection, or sequestration /repair of potentially toxic hydrophobic molecules created by photo-oxidative stress, one would expect an increased amount of LDs as has been observed in high-light treated leaf chloroplasts (Lichtenthaler 2007). However we cannot rule out the possibility that reduced lipid production and storage caused by high-light damage is counterbalanced by increases in LD storage of damaged thylakoid lipids.

Due to the ability to produce nitrogen-fixing heterocysts (Meeks et al. 2002), LD production cannot be stimulated by nitrogen starvation as in algae (Wang et al. 2009), however it is obvious that LD formation changes with the type of nitrogen provided for exponential growth (Fig. 2). Readily assimilated ammonia from the media or glutamine provided to vegetative cells by nitrogen-fixing heterocysts (Wolk et al. 1994), results in the lowest level of LD production during exponential growth whereas nitrate, which requires significant input of reducing power by cells for its assimilation results in higher levels of LD production. The reason for this is unknown, but may indicate the involvement of carbon/nitrogen or redox balance in the regulation of LD formation. Expression of LDs increases during stationary phase regardless of the nitrogen source used during exponential growth (Fig. 2). This is similar to increased glycogen accumulation observed as cyanobacteria enter stationary phase when some factor other than carbon is limiting. Cells grown with exogenous sugar also exhibit stationary-like levels of expression during exponential growth, indicating that LDs in *N. punctiforme* may function as storage reservoirs for carbon. Late stationary phase cells had the most LDs and log phase had the least. This observation also supports a role for LDs as an internal energy source for re-entering active growth.

Isolation of a buoyant cell fraction enriched for LDs that were visibly free of cells and thylakoid membranes (Fig. 1D & E) allowed identification of lipids enriched in cyanobacterial LDs. As the focus of this work was on uncharged lipid containing bodies, we

concentrated on neutral lipid analysis by utilizing methods that assured neutral lipid extraction and separation. GC-MS analysis of excised TLC spots containing two enriched LD lipids identified TAG and -tocopherol (Fig. 3). Saponification and derivatization of the excised TAG spot and subsequent FAME analysis indicated TAG is composed of only saturated C16:0 and C18:0 fatty acids constituents. Thus, it is likely that the increased TAG in LDs give rise to the enrichment of these saturated FAMEs obtained from purified LDs (Figure 4B & C). TAG with saturated fatty acids would pack tightly and be a compact storage molecule. - Tocopherol (vitamin E) is an antioxidant able to stop peroxidation of unsaturated membrane lipids (Havaux et al. 2005) and its identification in isolated LDs indicate they my have a similar role in cyanobacteria. Enzymes catalyzing its synthesis were also found enriched in chloroplast PGs and used to invoke active participation of PGs in metabolism and repair rather than being simple reservoirs for lipids (Vidi et al. 2006).

Although not visualized well on the TLC plate, a C17 alkane was also found to be enriched in isolated LDs (Fig. 4B & C), especially in exponentially growing cells (Fig. 4B). The presence of alkanes has previously been reported for *N. punctiforme* and the two genes encoding enzymes required for its synthesis identified (Schirmer et al. 2010). Since alkanes are extremely hydrophobic, it is not surprising to see them accumulate in LDs. It will be interesting to see if the enzymes catalyzing the decarboxylation of fatty acids into alkanes are localized at or near LDs.

Based upon the low level of green chlorophyll pigments visible on TLC lanes containing purified LD samples, the non-polar lipids near the origin (Fig. 3) likely originated from those composing LDs and are not due to contaminating thylakoid membranes. Since the interior of LDs is proposed to be extremely hydrophobic, the head-groups of non-polar lipids and - tochopherol would be expected to be part of the exterior surface lipid monolayer as has been proposed for the general model of LD structure (Murphy 2012). The enrichment for TAG with saturated fatty acids and C17 alkanes in cyanobacterial LDs (Fig. 4B) make these the logical components residing in the internal hydrophobic core. The reason that LD fatty acid composition changes to include saturated species more typical of whole cells during stationary phase (Fig. 4C) could reflect LDs act as a reservoir for storage or recycling of thylakoid membranes during under this growth condition. Such a role has been hypothesized for chloroplast plastoglobules during chloroplast senescence (Besagni and F. 2013).

To our knowledge this is the first report of the occurrence of large neutral lipid-containing structures visible with the light microscope in cyanobacteria. The finding that a C17 alkane and TAG containing saturated fatty acids are enriched in these easy to isolate lipid “packages” has the potential for biotechnological applications if LD production could be increased. The finding that LD expression and fatty acid composition is altered with changing growth conditions and the finding of an anti-oxidant molecule indicates the role of cyanobacterial LDs may be complex and multifunctional. Future identification of proteins associated with these structures and creation of mutants lacking or over-expressing LDs will certainly aid in understanding the physiological role of these novel cyanobacterial structures. To truly achieve “green fuel” or high value lipids/lipid-soluble products in the future, a basic understanding of lipid droplet composition, formation and function will be required to form

the physiological and metabolic engineering strategies required to advance expression of microalgae-based production systems.

Acknowledgments

This work was supported by National Institutes of Health Grant 5SC1GM093998, National Science Foundation Grant MCB-1413583, and funding from California State University for Education and Research in Biotechnology (CSUPERB) to MLS.

References

Allen M, Arnon DI. Studies on nitrogen-fixing blue-green algae. I. Growth and nitrogen fixation by *Anabaena cylindrica* Lemm. Plant Physiol. 1955; 30:366–372. [PubMed: 16654787]

Austin JR, Frost E, Vidi P-A, Kessler F, Staehelina LA. Plastoglobules are lipoprotein subcompartments of the chloroplast that are permanently coupled to thylakoid membranes and contain biosynthetic enzymes. Plant Cell. 2006; 18:1693–1703. [PubMed: 16731586]

Besagni C, Kessler F. A mechanism implicating plastoglobules in thylakoid disassembly during senescence and nitrogen starvation. Planta. 2013; 237:463–470. [PubMed: 23187680]

Bligh E, Dyer WJ. A rapid method of total lipid extraction and purification. Canadian J. Biochem Physiol. 1959; 37:911–917.

Boudière L, et al. Glycerolipids in photosynthesis: Composition, synthesis and trafficking. Biochim et Biophys Acta (BBA) - Bioenergetics. 2014; 1837:470–480.

Bréhélin C, Kessler F. The plastoglobule: A bag full of lipid biochemistry tricks. Photochem Photobiol. 2008; 84:1388–1394. [PubMed: 19067960]

Chapman KD, Dyer JD, Mullen RT. Biogenesis and functions of lipid droplets in plants. J. Lipid Res. 2012; 53:215–226. [PubMed: 22045929]

Cooper MS, Hardin WR, Petersen TW, Cattolico RA. Visualizing “green oil” in live algal cells. J Biosci Bioeng. 2010; 109:198–201. [PubMed: 20129108]

Cunningham FX, Tice AB, Pham C, Gantt E. Inactivation of genes encoding plastoglobulin-like proteins in *Synechocystis* sp. PCC 6803 leads to a light-sensitive phenotype. J Bacteriol. 2010; 192:1700–1709. [PubMed: 20081034]

Deruere J, Romer S, d'Harlingue A, Backhaus R, Kuntz M, Camara B. Fibril assembly and carotenoid overaccumulation in chromoplasts: A model for supramolecular lipoprotein structures. Plant Cell. 1994:119–133. [PubMed: 8130642]

Ding Y, et al. Identification of the major functional proteins of prokaryotic lipid droplets. J. Lipid Res. 2012; 53:399–411. [PubMed: 22180631]

Edwards MR, Berns DS, Ghiorse WC, Holt SC. Ultrastructure of the thermophilic blue-green alga, *Synechococcus lividus* Copeland. J Phycol. 1968; 4:283–298.

Fan J, Yan C, Andre C, Shanklin J, Schwender J, Xu C. Oil accumulation is controlled by carbon precursor supply for fatty acid synthesis in *Chlamydomonas reinhardtii*. Plant Cell Physiol. 2012; 53:1380–1390. [PubMed: 22642988]

Farese RVJ, Walther TC. Lipid droplets finally get a little R-E-S-P-E-C-T. Cell. 2009; 139:855–860. [PubMed: 19945371]

Goodson C, Wang ZT, Goodenough U. Structural correlates of cytoplasmic and chloroplast lipid body synthesis in *Chlamydomonas reinhardtii* and stimulation of lipid body production with acetate boost. Eukaryot Cell. 2011; 10:1592–1606. [PubMed: 22037181]

Havaux M, Eymery F, Porfirova S, Pascal Rey P, Peter Dörmann P. Vitamin E protects against photoinhibition and photooxidative stress in *Arabidopsis thaliana*. Plant Cell. 2005; 17:3451–3469. [PubMed: 16258032]

Hu Q, et al. Microalgal triacylglycerols as feedstocks for biofuel production: perspectives and advances. Plant J. 2008; 54:621–639. [PubMed: 18476868]

Hutchins PM, Barkley RM, Murphy RC. Separation of cellular nonpolar neutral lipids by normal-phase chromatography and analysis by electrospray ionization mass spectrometry. J. Lipid Res. 2008; 49:804–813. [PubMed: 18223242]

Jacquier N, Mishra S, Choudhary V, Schneiter R. Expression of oleosin and perilipins in yeast promote formation of lipid droplets from the endoplasmatic reticulum. J Cell Sci. 2013; 126:5198–5209. [PubMed: 24006263]

Kessler F, Vidi P-A. Plastoglobule lipid bodies: their functions in chloroplasts and their potential for applications. Adv Biochem Engin/Biotechnol. 2007; 107:153–172.

Khandelia H, Duelund L, Pakkanen KI, Ipsen JH. Triglyceride blisters in lipid bilayers: implications for lipid droplet biogenesis and the mobile lipid signal in cancer cell membranes. PLoS ONE. 2010; 5:e12811. [PubMed: 20877640]

Kuroiwa T, et al. Lipid droplets of bacteria, algae and fungi and a relationship between their contents and genome sizes as revealed by BODIPY and DAPI staining. Cytologia. 2012; 77:289–299.

Lichtenthaler HK. Biosynthesis, accumulation and emission of carotenoids, α-tocopherol, plastoquinone, and isoprene in leaves under high photosynthetic irradiance. Photosynth Res. 2007; 92:163–179. [PubMed: 17634750]

Maeda K, et al. Adipocyte/macrophage fatty acid binding proteins control integrated metabolic responses in obesity and diabetes. Cell Metab. 2005; 1:107–119. [PubMed: 16054052]

Meeks JC, Campbell EL, Summers ML, Wong FC. Cellular differentiation in the cyanobacterium *Nostoc punctiforme*. Arch Microbiol. 2002; 178:395–403. [PubMed: 12420158]

Miao XL, Wu QY. Biodiesel production from heterotrophic microalgal oil. Bioresource Tech. 2006; 97:841–846.

Moellering, ER.; Miller, R.; Benning, C. Molecular genetics of lipid metabolism in the model green alga *Chlamydomonas reinhardtii*.. In: Wada, H.; Murata, M., editors. Lipids in Photosynthesis: Essential and Regulatory Functions. Springer; Dordrecht: 2009. p. 139-150.

Murphy DJ. The dynamic roles of intracellular lipid droplets: from archaea to mammals. Protoplasma. 2012; 249:541–585. [PubMed: 22002710]

Murphy DJ, Vance J. Mechanisms of lipid-body formation. TIBS. 1999; 24:109–115. [PubMed: 10203758]

Nierswicki-Bauer SA, Balkwill DL, Stevens SE Jr. Three-dimensional ultrastructure of a unicellular cyanobacterium. J Cell Biol. 1983; 97:713–722. [PubMed: 6411738]

Pankratz HS, Bowen CC. Cytology of blue-green algae. I. The cells of *Symploca muscorum*. Amer J Bot. 1963; 50:387–399.

Piller LE, Abraham M, Dormann P, Kessler F, Besagni C. Plastid lipid droplets at the crossroads of prenylquinone metabolism. J Exper Bot. 2012; 63:1609–1618. [PubMed: 22371323]

Rey P, et al. Over-expression of a pepper plastid lipid-associated protein in tobacco leads to changes in plastid ultrastructure and plant development upon stress. Plant J. 2000; 21:483–494. [PubMed: 10758499]

Schirmer A, Rude MA, Li X, Popova E, del Cardayre SB. Microbial biosynthesis of alkanes. Science. 2010; 329:559–562. [PubMed: 20671186]

Selvan BK, Revathi M, Piriya PS, Vasan PT, Prabhu DIG, Vennison SJ. Biodiesel production from marine cyanobacteria culture in plate and tubular photobioreactors. Ind J Exp Biol. 2013; 51:262–268.

Sheng J, Vannela R, Rittmann BE. Evaluation of methods to extract and quantify lipids from *Synechocystis* PCC 6803. Bioresource Tech. 2011; 102:1697–1703.

van de Meene AML, Hohmann-Marriott MF, Vermaas WFJ, Roberson RW. The three-dimensional structure of the cyanobacterium *Synechocystis* sp. PCC 6803. Arch Micrbiol. 2006; 184:259–270.

Vidi P-A, et al. Tocopherol cyclase (VTE1) localization and vitamin E accumulation in chloroplast plastoglobule lipoprotein particles. J Biol Chem. 2006; 281:11225–11234. [PubMed: 16414959]

Wang ZT, Ullrich N, Joo S, Waffenschidt S, Goodenough U. Algal lipid bodies: Stress induction, purification, and biochemical characterization in wild-type and starchless *Chlamydomonas reinhardtii*. Eukaryot Cell. 2009; 8:1856–1868. [PubMed: 19880756]

Wolk CP. Physiology and cytological chemistry of blue-green algae. Bacteriol Rev. 1973; 37:32–101. [PubMed: 4633592]

Wolk, CP.; Ernst, A.; Elhai, J. Heterocyst Metabolism and Development.. In: Bryant, DA., editor. The Molecular Biology of Cyanobacteria. Kluwer Acad Publ.; Dordrecht, The Netherlands: 1994. p. 769-823.

Yang L, et al. The proteomics of lipid droplets: structure, dynamics, and functions of the organelle conserved from bacteria to humans. J Lipid Res. 2012; 53:1245–1253. [PubMed: 22534641]

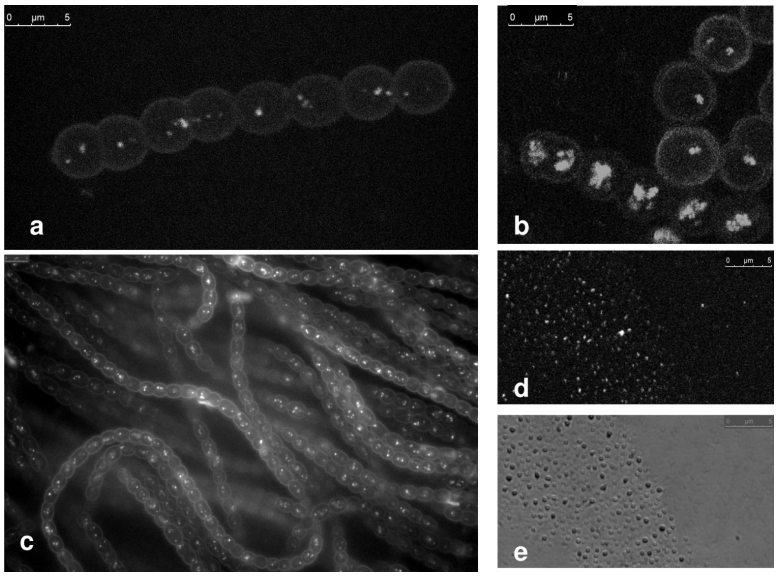

Fig.1.

Staining and visualization of cyanobacterial lipid droplets (LDs). **a** MOPS/Ammonia grown cells showing LDs stained with BODIPY *in vivo* and visualized using confocal microscopy. **b** Late stationary phase MOPS/Ammonia/Fructose grown cells showing LDs stained with BODIPY. **c** MOPS/Ammonia grown cells stained with HCS LipidTOX green neutral lipid stain. **d** Stained neutral lipid droplets with BODIPY following purification. **e** Bright field image of lipid droplets shown in d

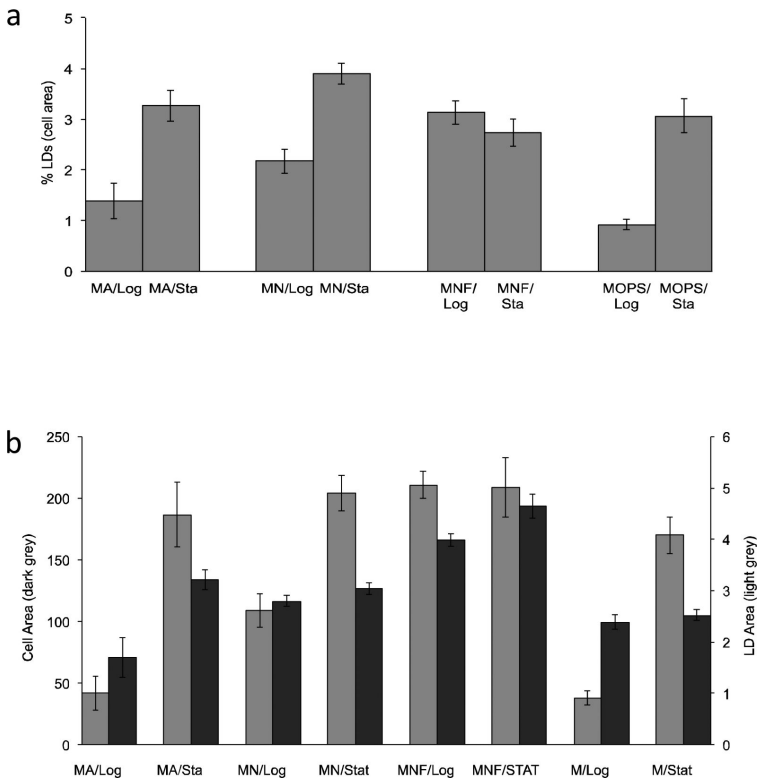

Fig. 2.

LD and cell area comparisons. **a** Percent LD area per cell (n >100) determined from BODIPY stained confocal Z-stack projection images. **b** Raw data (pixels) for cell area and LD area used in a. Cultures were grown in MOPS/Ammonia (MA), MOPS/Nitrate (MN), MOPS/Nitrate/Fructose (MNF) or under nitrogen-fixing conditions with MOPS buffer only (M). Cells were measured during log phase (Log; 3.8-5.1 g Chla/ml) and during stationary phase (Sta; 31-50 g Chla/ml). MA stationary phase cultures were initially grown with ammonia, then allowed to transition to nitrogen fixing growth conditions when the ammonia was depleted from batch cultures

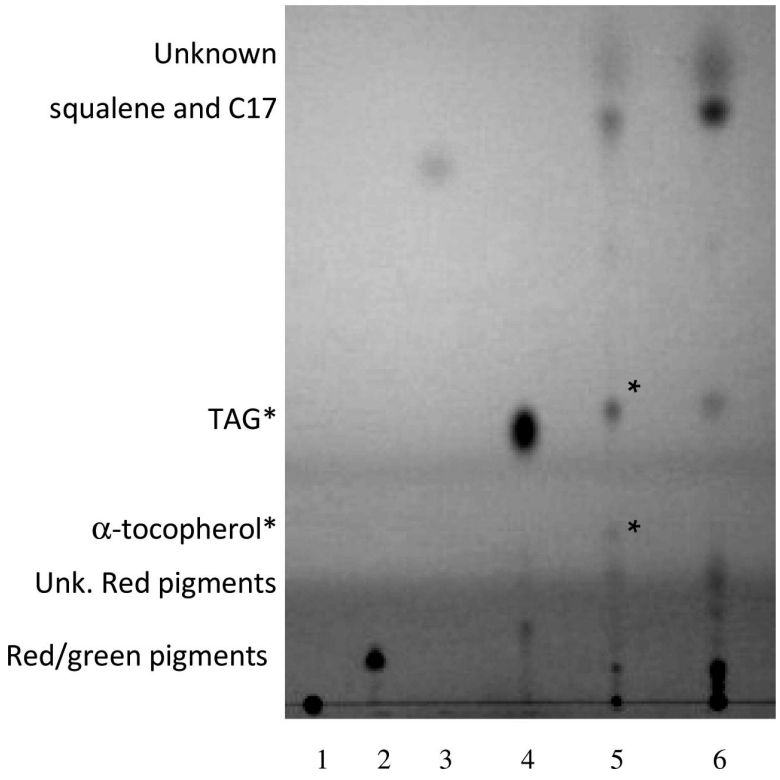

Fig. 3.

TLC separation of lipids. Lane 1. Charged lipid standard (1,2-Distearoyl-*sn*-Glycero-3-[Phospho-rac-1-glycerol]), 2. Diacylglycerol (DAG) standard, 3. Butylated hydroxytoluene standard, 4. Triacylglycerol standard, 5. Neutral lipids from the lipid droplet enriched fraction, 6. Neutral lipids from the ultracentrifuge pellet. Cell samples contained in lanes 5 & 6 were obtained from stationary phase cultures initial grown in MOPS/Ammonia. Observations or identifications based on GC-MS analysis of biological samples shown at left. Relative spot intensities within each sample shown at right. Asterisks denotes lipids enriched in cyanobacterial LDs

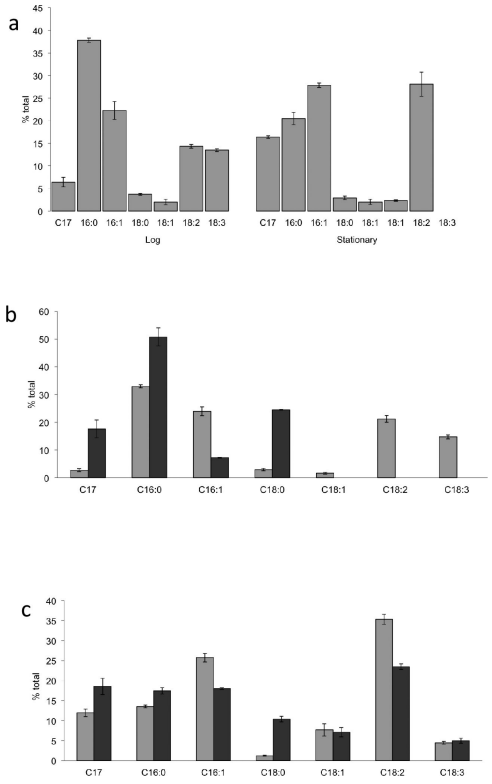

Fig. 4.

Relative percent of heptadecane and FAMEs extracted from whole cells (**a**), or from lipid droplet enriched fraction and debris pellets from exponentially grown (**b**) or stationary (**c**) phase cultures. FAMEs and heptadecane obtained from cell pellet fraction or whole cells (light gray) and isolated LDs (dark gray). Lipids were extracted from MA grown culture during exponential growth or from late stationary phase cultures initially grown in MA that had transitioned to nitrogen-fixing growth (n=3).